Università degli Studi di Palermo

AREA RICERCA E INNOVAZIONE
SETTORE DOTTORATI E CONTRATTI PER LA RICERCA
U. O. DOTTORATI DI RICERCA

PhD School in Biomedicine, Neuroscience and Advanced Diagnostic
Department of Biomedicine, Neuroscience and Advanced Diagnostic (Bi.N.D.)
SSD: MED/36

Multiparametric evaluation in patients with non-alcoholic fatty liver disease (NAFLD) using quantitative imaging: an integrated approach for risk stratification

THE DOCTOR
Domenico Salvatore Gagliano

THE COORDINATOR
Prof. Fabio Bucchieri

THE TUTOR
Prof. Giuseppe Brancatelli

XXXVIII Cycle
Academic year 2022-2023

INDEX

1. Introduction

1.1 From NAFLD to MASLD (Metabolic Dysfunction–Associated Steatotic Liver Disease): definitions, diagnostic criteria and global burden

Nonalcoholic fatty liver disease (NAFLD) is a chronic liver disorder characterized by excessive hepatic fat accumulation in the absence of significant alcohol intake or other secondary causes of steatosis. It is closely associated with metabolic dysfunction, encompassing obesity, insulin resistance, type 2 diabetes mellitus, dyslipidemia, and arterial hypertension, and currently represents the most prevalent cause of chronic liver disease worldwide with a global prevalence of 30% (Figure 1) (1,2).

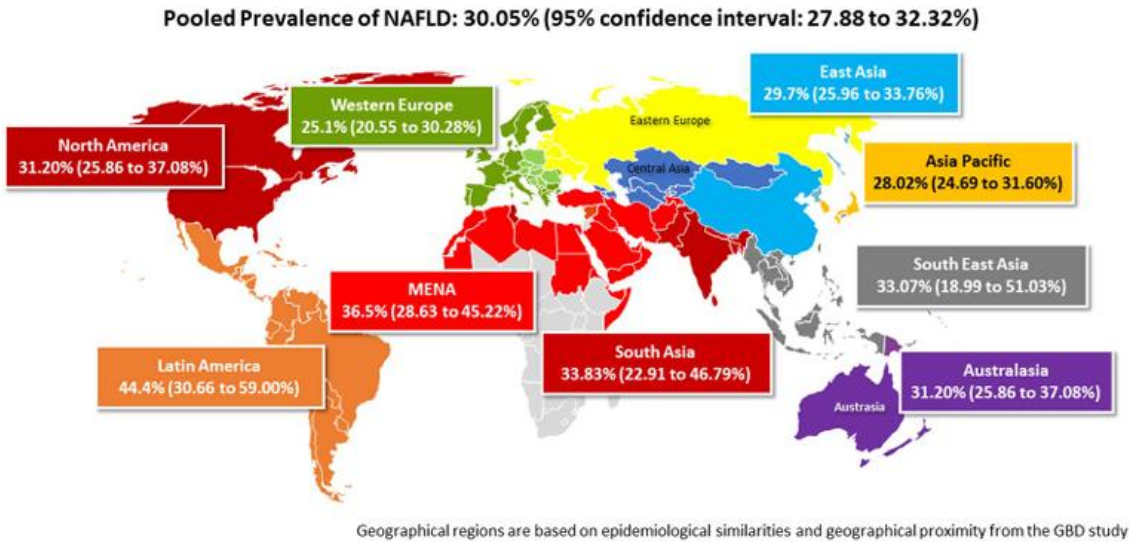

Figure 1 - Prevalence of NAFLD According to Global Regions Data Collected 1990–2019 (1).

From a clinical and pathophysiological perspective, NAFLD is not a single entity but rather a heterogeneous disease spectrum with a highly variable natural history and clinical outcomes (3,4).

The NAFLD spectrum ranges from isolated hepatic steatosis, also referred to as nonalcoholic fatty liver (NAFL), to nonalcoholic steatohepatitis (NASH), the progressive inflammatory phenotype. NASH is histologically defined by the coexistence of steatosis, hepatocellular ballooning, lobular inflammation, and variable degrees of fibrosis (5,6).

Unlike simple steatosis, NASH is associated with a markedly increased risk of progression to advanced fibrosis, cirrhosis, hepatocellular carcinoma, and liver-related mortality (7).

The pathogenesis of NAFLD is complex and multifactorial, exceeding the scope of a single pathogenic mechanism. The currently accepted "multiple-hit" model integrates the synergistic effects of systemic and hepatic insulin resistance, increased free fatty acid (FFA) flux to the liver, enhanced *de novo* lipogenesis, mitochondrial dysfunction, oxidative stress, and endoplasmic reticulum stress, ultimately leading to hepatocellular injury and the activation of inflammatory and fibrogenic pathways (8–10). Genetic susceptibility plays a pivotal modulatory role, with variants in genes such as *PNPLA3* influencing hepatic fat accumulation and fibrosis progression (11). In addition, alterations in the gut–liver axis, including intestinal dysbiosis and increased gut permeability, contribute to hepatic inflammation and disease progression (10,12).

Clinically, NAFLD is often asymptomatic, particularly in its early stages, and is frequently detected incidentally through imaging studies or mild abnormalities in liver enzymes. However, serum aminotransferase levels (ALT/AST) are unreliable indicators of disease severity and may remain within normal ranges even in patients with advanced fibrosis (6,13). Consequently, identifying patients at risk of disease progression remains a critical unmet clinical need.

Recognizing the limitations of the "nonalcoholic" descriptor—which relies on a diagnosis of exclusion and carries a perceived social stigma—an international expert consensus has recently driven a paradigm shift in nomenclature.

The term metabolic dysfunction–associated steatotic liver disease (MASLD) has replaced NAFLD, while the progressive inflammatory phenotype is now redefined as metabolic dysfunction–associated steatohepatitis (MASH) (14,15). This transition emphasizes the affirmative role of metabolic drivers rather than the absence of alcohol (14). Under this refined framework, MASLD is defined by the presence of hepatic steatosis, detected by imaging or histology, in individuals with at least one of the following five cardiometabolic risk factor: increased body mass index (BMI) or waist circumference, impaired fasting glucose or diabetes, hypertension, low HDL cholesterol, or hypertriglyceridemia (6,15).

Furthermore, the new classification introduced the category of MetALD (Metabolic and Alcohol-related Liver Disease), which describes individuals meeting MASLD criteria who also consume moderate amounts of alcohol (30–60 g/day for men and 20–50 g/day for women). This category acknowledges the frequent synergy between metabolic dysfunction and alcohol intake, which was previously a "gray zone" in NAFLD definitions (14,15).

The broader spectrum of steatotic liver disease (SLD) also includes Alcohol-associated Liver Disease (ALD), where liver steatosis is attributed solely to alcohol intake (>60 g/day in men and >50 g/day in women), and SLD of specific etiologies such as drug-induced liver injury (e.g. corticosteroids, methotrexate, or tamoxifen), iron overload, or monogenic disorders (lysosomal acid lipase deficiency, hypobetalipoproteinemia, Wilson

disease), endocrine disorders, genotype 3 hepatitis C virus infection, autoimmune hepatitis, coeliac disease, malnutrition, or HIV infection (6).

Cases that do not meet any of these criteria are classified as cryptogenic SLD (Figure 2).

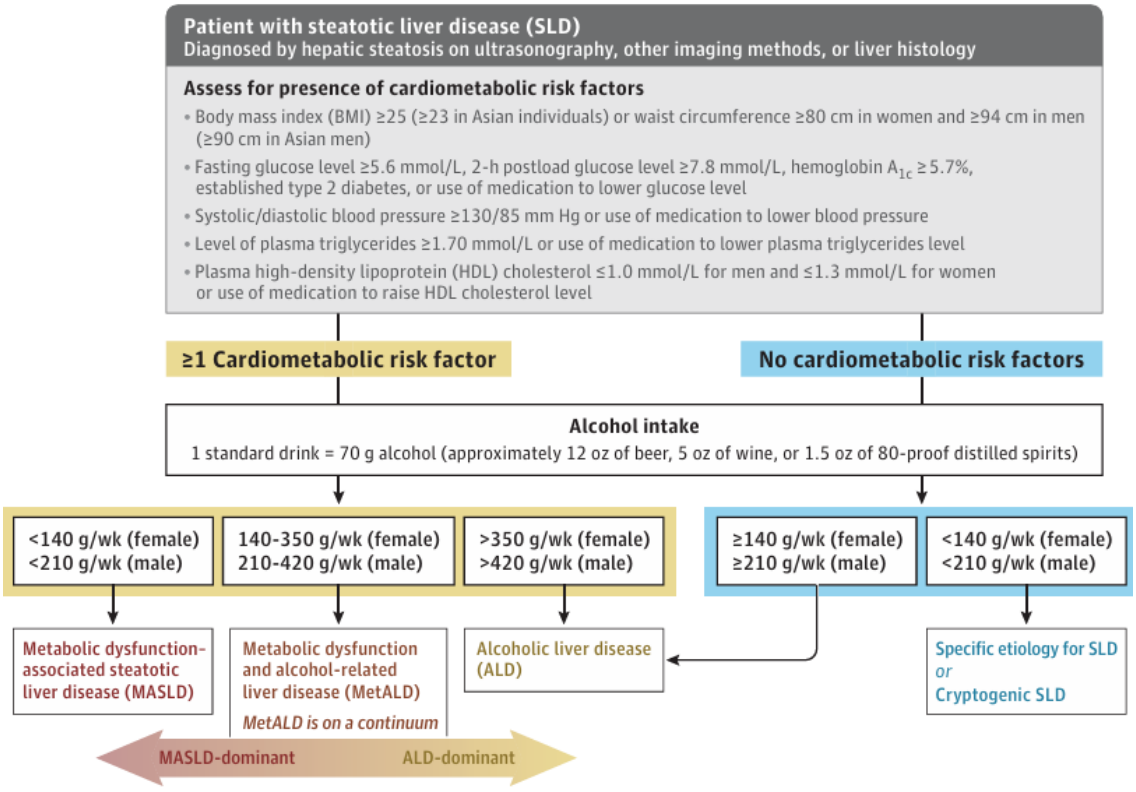

Figure 2 – Flowchart showing the classification and subclassification of steatotic liver disease (4).

MASLD represents the most common chronic liver disease globally, with an estimated prevalence of approximately 30–35% in the adult population, rising to more than 60% among individuals with obesity or type 2 diabetes mellitus (2,16).

Epidemiological data indicate a steady increase in prevalence over recent decades, paralleling the global rise in obesity and metabolic syndrome. Sex-related differences

have been observed, with higher prevalence in men; however, this difference diminishes after menopause, suggesting a modulatory role of sex hormones and fat distribution (17).

From a histopathological standpoint, MASLD encompasses a broad spectrum ranging from isolated steatosis to MASH, progressive fibrosis, cirrhosis, and its complications such as hepatocellular carcinoma development (Figure 3) (18).

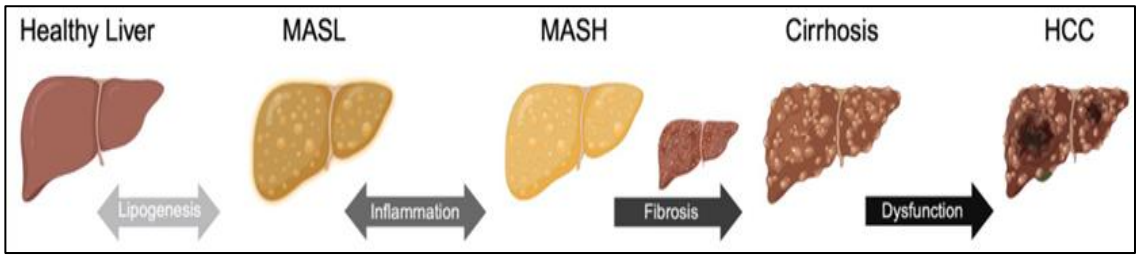

Figure 3 - Progression MASLD. It should be noted that the early stages are reversible (double-headed arrows), reflecting the need for early diagnosis and treatment. The onset of fibrosis marks the beginning of irreversible stages (single-headed arrows) that can lead to hepatocellular carcinoma (HCC) (18).

Although most individuals with MASLD do not always progress to advanced liver disease, a clinically relevant subset develops progressive fibrosis. Across multiple cohorts and meta-analyses, fibrosis stage consistently emerges as the dominant determinant of long-term prognosis (19–21).

MASLD is increasingly recognized as a systemic disease rather than a purely hepatic condition. Cardiovascular disease represents the leading cause of mortality among affected individuals, followed by extrahepatic malignancies (i.e. gastrointestinal, breast and gynecologic cancer) and liver-related complications (4,6,22).

This systemic burden underscores the importance of a multidisciplinary approach and firmly establishes MASLD as a major and growing global public health challenge.

1.2 Metabolic and clinical basis of hepatic steatosis

1.2.1 Liver structure and function

The liver plays a central role in systemic metabolic homeostasis, integrating carbohydrate, lipid, and protein metabolism. Its unique dual blood supply, derived from the portal vein and hepatic artery, exposes hepatocytes to nutrients, hormones, and metabolites originating from the intestine and peripheral tissues. This anatomical and functional organization underlies the liver's capacity to regulate energy storage and distribution in response to nutritional status (23).

Beyond its macroscopic architecture, the liver exhibits a marked degree of spatial metabolic heterogeneity, a phenomenon known as metabolic zonation. Hepatocyte specialization along the porto-central axis of the hepatic lobule establishes distinct metabolic microenvironments. Periportal hepatocytes (Zone 1) predominantly sustain oxidative phosphorylation, ureagenesis, and gluconeogenesis, whereas pericentral hepatocytes (Zone 3) are enriched in glycolytic enzymes, lipogenic pathways, and xenobiotic metabolism (24) (Figure 4).

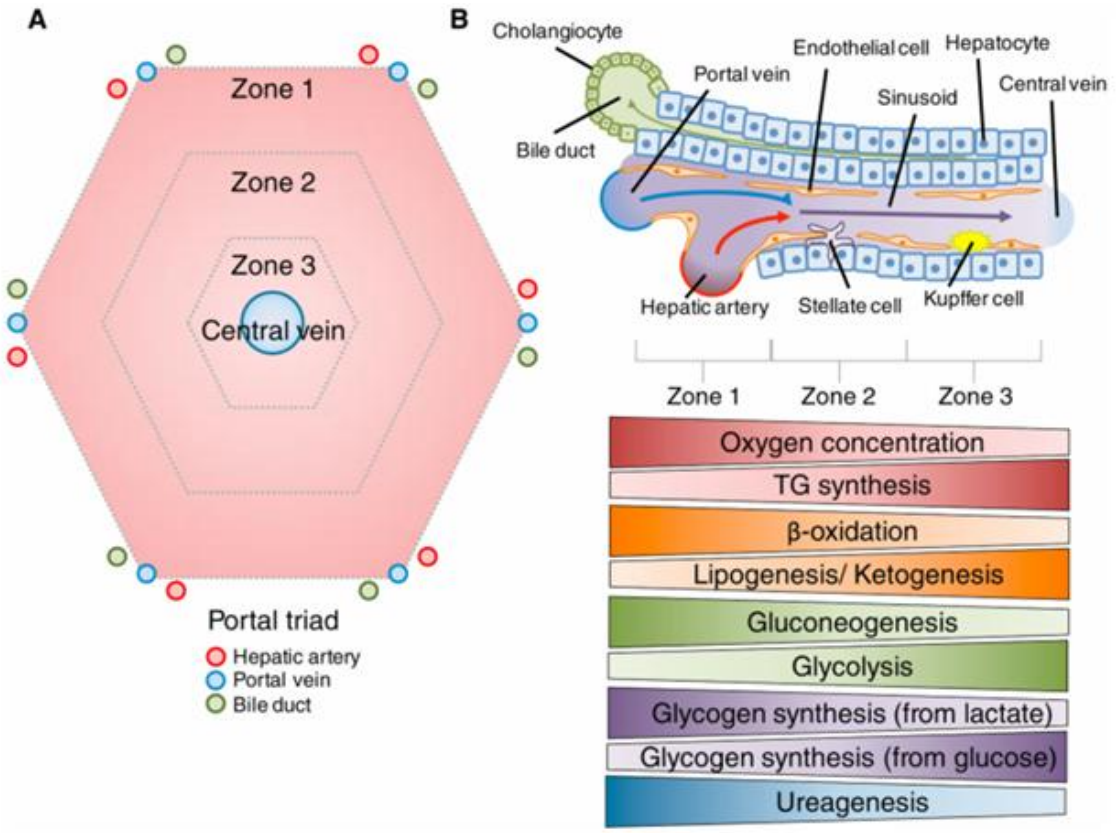

Figure 4 – Organization of the liver. (A) Geometric representation of a hepatic lobule. (B) A schematic representation of a sinusoid within the liver and the corresponding zonation of several metabolic processes across the sinusoid (23).

While classical descriptions of zonation derive from earlier experimental work, recent studies emphasize that this functional compartmentalization is dynamically regulated by gradients in oxygen tension, the Wnt/β-catenin signaling pathway, and nutrient availability (25). Such plasticity implies that metabolic stressors may differentially affect specific hepatocyte populations, predisposing pericentral regions to early lipid accumulation and oxidative injury, which are hallmarks of MASH.

In normal physiology, hepatic lipid content is tightly regulated through the balance between fatty acid uptake, *de novo* lipogenesis, mitochondrial β-oxidation, and the export of triglycerides in very-low-density lipoproteins (VLDL). This balance is not static but continuously modulated by insulin signalling, glucagon activity, and transcriptional regulators such as SREBP-1c and PPARα (26,27). Disruption of this balance, particularly in the setting of insulin resistance and excess caloric intake, leads to pathological lipid accumulation within hepatocytes, providing the biological substrate for hepatic steatosis.

1.2.2 Pathophysiology and clinical consequences

Hepatic steatosis arises from an imbalance between lipid acquisition and disposal within the liver. In the context of metabolic dysfunction, increased adipose tissue lipolysis leads to an elevated flux of free fatty acids (FFA) to the liver, representing the dominant source of hepatic triglycerides in steatotic liver disease (28). This mechanism, driven by adipose tissue insulin resistance, results in a continuous flooding of the liver with FFAs, particularly in patients with type 2 diabetes mellitus, where the prevalence of MASLD is estimated to exceed 70% (16). Concurrently, hyperinsulinemia and insulin resistance stimulate hepatic *de novo* lipogenesis while impairing fatty acid oxidation, further promoting lipid accumulation (29).

The accumulation of triglycerides within hepatocytes in the form of macrovesicular steatosis has traditionally been regarded as a relatively inert storage mechanism, serving as a cytoprotective buffer aimed at sequestering lipotoxic non-esterified fatty acid species. However, when the hepatic capacity to store or export lipids is overwhelmed, it triggers the generation of toxic lipid intermediates, most notably ceramides, diacylglycerols (DAGs), and lysophosphatidylcholine. This state, termed lipotoxicity, directly promotes organelle dysfunction (30). These molecules interfere with insulin signalling pathways, alter mitochondrial dynamics, and activate inflammatory cascades through oxidative and endoplasmic reticulum stress, which collectively contribute to hepatocellular injury and inflammatory signalling (7).

Moreover, emerging data challenge overly linear models of pathogenesis. Instead of a simple progression from fat accumulation to inflammation, metabolic stress appears to induce parallel alterations in mitochondrial bioenergetics, redox signalling, and

hepatocellular immune responses. This multidimensional framework helps explain why some individuals with substantial steatosis remain clinically stable, whereas others progress toward steatohepatitis and fibrosis (7).

While simple steatosis has historically been viewed as a benign condition, increasing evidence suggests that it is not entirely innocuous and is recognized as part of a broader cardiometabolic risk spectrum. Hepatic steatosis creates a permissive metabolic and inflammatory environment that may facilitate disease progression in susceptible individuals. Factors such as genetic predisposition (particularly the PNPLA3 I148M variant), persistent insulin resistance, and alterations in the gut–liver axis modulate the transition from steatosis to steatohepatitis and fibrosis (8,31).

From a systemic standpoint, liver functions not only as a target organ but also as a sensor of systemic metabolic stress and liver fat content reflects whole-body metabolic health and risk. Hepatic steatosis indeed is associated with increased cardiovascular risk and adverse metabolic outcomes, independent of liver-specific complications.

Importantly, hepatic steatosis represents a dynamic and potentially reversible process. Changes in dietary intake, physical activity, and insulin sensitivity can rapidly modulate liver fat content, distinguishing steatosis from more advanced and structurally fixed disease stages such as fibrosis. This dynamic nature distinguishes steatosis from later fibrotic stages and provides the biological basis for its use as a responsive biomarker for both disease monitoring and therapeutic assessment.

1.2.3 Therapeutic implications

Hepatic steatosis represents a dynamic and potentially reversible component of metabolic liver disease, making it a clinically relevant target for therapeutic interventions. Lifestyle modification, including caloric restriction, optimization of dietary composition, and increased physical activity, remains the cornerstone of management and has been consistently associated with significant reductions in liver fat content. Importantly, improvements in steatosis often precede measurable changes in hepatic inflammation and fibrosis, highlighting its sensitivity as an early marker of metabolic response (32).

Beyond lifestyle interventions, novel pharmacological strategies targeting insulin resistance, lipid metabolism, and energy homeostasis - most notably GLP-1 receptor agonists and dual GIP/GLP-1 agonists - have demonstrated a potent ability to reduce hepatic fat accumulation (33). Although most pharmacological treatments are currently reserved for selected patient populations and specific disease stages, the recent approval of the first MASH-specific therapy (Resmetirom) and the results from late-stage clinical trials (34) further support the concept of hepatic steatosis as a modifiable and clinically significant therapeutic target.

In patients with severe obesity and metabolic dysfunction, bariatric surgery represents an effective therapeutic option with profound metabolic effects (35). Surgical weight-loss interventions have been associated with marked and sustained reductions in hepatic steatosis, as well as improvements in steatohepatitis and fibrosis in a substantial proportion of patients. These effects further emphasize the close link between systemic metabolic health and liver fat content, and underscore the responsiveness of hepatic steatosis to interventions that induce significant metabolic remodelling (35).

The reversibility and temporal variability of hepatic steatosis underscore the limitations of static or invasive assessment methods and reinforce the need for quantitative, non-invasive tools capable of capturing longitudinal changes. Accurate measurement of liver fat content is therefore essential, not only for disease characterization but also for monitoring therapeutic response and informing risk-adapted clinical management strategies. In this clinical landscape, the transition toward non-invasive quantification is no longer merely a diagnostic preference but a fundamental requirement for assessing the efficacy of emerging metabolic therapies.

1.3 From metabolic marker to multiparametric imaging assessment

Although hepatic steatosis is not the primary determinant of liver-related outcomes, it represents a robust biomarker of systemic metabolic dysfunction. Hepatic fat accumulation is strongly associated with obesity, type 2 diabetes mellitus, dyslipidemia, and insulin resistance, reflecting the central role of the liver in metabolic homeostasis (36).

Clinically, steatosis is highly prevalent, often precedes the development of necroinflammation and fibrosis, and remains sensitive to metabolic perturbations. For these reasons, changes in liver fat content are frequently used as early indicators of therapeutic response, as reductions in steatosis typically occur before measurable improvements in inflammatory activity or fibrosis (37).

Despite these advantages, steatosis is an imperfect biomarker when considered in isolation. Its presence does not reliably predict progression to advanced liver disease, and its absence does not exclude significant fibrosis. This apparent paradox highlights the need for integrated assessment strategies that capture multiple dimensions of disease biology rather than relying on a single parameter. Consequently, the accurate and longitudinal quantification of hepatic steatosis should be interpreted within a broader multiparametric framework that incorporates structural and functional information.

The need for such an approach is reinforced by the limitations of conventional diagnostic and prognostic tools in MASLD. Liver biopsy has traditionally been regarded as the reference standard for evaluating steatosis, inflammation, and fibrosis; however, its invasive nature, associated risks, limited patient acceptance, and unsuitability for repeated

assessments restrict its clinical applicability, particularly in a condition characterized by slow progression and long-term follow-up requirements (38). In addition, sampling variability and interobserver may lead to the misclassification of disease severity and hinder accurate monitoring of temporal changes.

Serum-based biomarkers and composite fibrosis scores, including the Fibrosis-4 (FIB-4) index and the NAFLD fibrosis score, are widely implemented in clinical practice. Although these tools demonstrate acceptable performance for excluding advanced fibrosis at the population level, their accuracy for individual risk stratification remains limited, especially in intermediate-risk groups (39). Moreover, serum biomarkers provide indirect information and do not allow the direct quantification of hepatic fat content or the assessment of intrahepatic spatial heterogeneity.

Conventional imaging techniques also present significant constraints. Qualitative B-mode ultrasonography is commonly used for detecting hepatic steatosis but is operator-dependent and lacks sensitivity for mild disease, as well as reproducibility for longitudinal monitoring (40).

Computed tomography (CT) can estimate hepatic fat content through attenuation measurements; however, radiation exposure and reduced sensitivity in early stages limit its routine use. Furthermore, qualitative or semi-quantitative methods are poorly suited to capturing the dynamic and heterogeneous nature of steatosis, which requires objective and continuous measurements over time.

Taken together, these limitations support the growing role of quantitative imaging biomarkers. Quantitative, non-invasive techniques provide standardized and reproducible measurements that enable a longitudinal assessment of disease burden, the early detection

of therapeutic response, and improved risk stratification. Within this context, the evaluation of hepatic steatosis becomes one component of a broader multiparametric imaging strategy aimed at integrating the metabolic, inflammatory, and fibrotic features of MASLD, thereby offering a more comprehensive representation of disease severity and progression.

2. Quantitative imaging in MASLD

2.1 MRI-Proton Density Fat Fraction as a quantitative reference standard

Magnetic resonance imaging–proton density fat fraction (MRI-PDFF) has emerged as the most accurate and reproducible non-invasive technique for the quantification of hepatic steatosis. PDFF represents the proportion of mobile protons attributable to fat relative to the total mobile proton density, expressed as a percentage. This provides a standardized and continuous measure of liver fat content that objectively reflects the histological grade of steatosis across the entire organ (41).

Multiple validation studies have demonstrated a strong correlation between MRI-PDFF and histological steatosis grade, with superior accuracy compared with other non-invasive imaging modalities, including conventional ultrasound and Controlled Attenuation Parameter (CAP) (42). Importantly, MRI-PDFF allows for whole-liver assessment, thereby overcoming the sampling limitations inherent to liver biopsy. Its high reproducibility and sensitivity to small changes in fat content have led to its widespread adoption as a surrogate endpoint in clinical trials targeting hepatic steatosis and metabolic dysfunction (37).

A key strength of MRI-PDFF lies in its cross-platform reproducibility and sensitivity to small longitudinal changes in liver fat. Technical validation studies have shown minimal bias across different magnetic field strengths (1.5T and 3T) and vendor platforms, supporting its robustness for multicenter trials and longitudinal monitoring (43).

This high precision explains why MRI-PDFF has been increasingly incorporated as a surrogate endpoint in pharmacological studies targeting steatosis reduction or metabolic dysfunction. Extensive data indicate that a relative reduction of approximately 30% in PDFF is a strong predictor of histological improvement in inflammatory activity or MASH resolution (44).

Despite its methodological advantages, MRI-PDFF remains limited by practical considerations that restrict its universal implementation. MRI examination's costs, scanner availability, duration, and contraindications such as implanted devices or severe claustrophobia reduce accessibility, particularly in large-scale screening settings or resource-limited environments. While meta-analytic evidence confirms excellent diagnostic performance, current guidelines generally position MRI-PDFF as a second-line quantitative reference rather than a population screening tool, emphasizing the need for complementary imaging biomarkers that balance accuracy with feasibility (45).

Consequently, alternative modalities—particularly point-of-care quantitative ultrasound techniques—are increasingly evaluated against MRI-PDFF as the non-invasive reference standard, reflecting its role as a methodological benchmark rather than a universally deployable frontline test.

2.2 Quantitative ultrasound techniques for the assessment of hepatic steatosis

Quantitative ultrasound (QUS) has gained increasing attention as a non-invasive, widely accessible approach for liver fat quantification. Unlike conventional B-mode imaging, QUS techniques are based on the analysis of the acoustic properties of liver tissue, providing objective and continuous measurements that are less dependent on operator interpretation.

The ultrasound attenuation coefficient (AC) represents one of the most robust quantitative parameters for non-invasive liver fat assessment, as it reflects the frequency-dependent reduction in ultrasound beam amplitude caused by absorption and scattering within hepatic tissue. Lipid accumulation increases acoustic attenuation by enhancing microscopic acoustic interfaces, producing a measurable slope of signal decay with depth that can be quantified in dB/cm/MHz. Compared with qualitative echogenicity assessment, attenuation-based metrics provide continuous measurements that enable an objective monitoring of steatosis severity and longitudinal changes.

Recent technical implementations by different ultrasound machines and brands—such as attenuation imaging (ATI), ultrasound-guided attenuation parameter (UGAP), and integrated attenuation (iATT)—rely on radiofrequency signal analysis and model-based compensation algorithms designed to reduce dependence on gain settings and beam geometry. Multicenter and prospective studies have demonstrated strong correlations between attenuation coefficient measurements and MRI-PDFF, with high diagnostic accuracy for detecting steatosis and good reproducibility across operators (46–48).

Another quantitative approach based on conventional B-mode data is the hepato-renal index (HRI), defined as the ratio between liver parenchymal echogenicity and right renal cortical echogenicity measured within matched regions of interest (ROIs). By normalizing liver brightness to the kidney, HRI aims to mitigate the inter-examination variability related to absolute gain and system settings, providing a simple surrogate of the steatosis-related increased echogenicity.

Recent prospective evidence in MASLD, including cohorts with type 2 diabetes, has shown that ultrasound HRI correlates with MRI-PDFF and can achieve clinically meaningful diagnostic performance for the detection of mild steatosis detection when MRI-PDFF is used as the reference standard (49).

Despite its simplicity and wide availability, the HRI presents several limitations; for instance, its use is not feasible in cases of right nephrectomy, as well as it could be unreliable in patients where renal parenchymal echogenicity is altered by chronic kidney disease or other nephropathies.

The controlled attenuation parameter (CAP), derived from vibration-controlled transient elastography (VCTE), represents a commercially available implementation of attenuation-based fat quantification. CAP has shown reasonable diagnostic performance for the detection of moderate-to-severe steatosis; however, its accuracy is reduced in obese individuals and in the presence of advanced fibrosis, and it lacks the spatial resolution provided by B-mode guidance (50).

Indeed, an important advantage of attenuation imaging and HRI over CAP is the ability to perform measurements under real-time B-mode guidance, allowing operators to avoid vessels, artifacts, and focal lesions during ROI placement.

Complementing attenuation-based parameters, shear wave elastography (SWE) provides mechanical information on liver tissue stiffness. Unlike attenuation imaging or HRI, which primarily target fat-related acoustic changes, SWE evaluates the propagation speed of mechanically induced shear waves within the hepatic parenchyma, allowing an estimation of tissue elasticity.

Liver stiffness, typically expressed in kPa, is strongly associated with hepatic fibrosis whereas the direct impact of steatosis on stiffness is generally limited.

Over the past decade, SWE has evolved into a multiparametric tool integrated into conventional ultrasound systems, including point SWE (pSWE) and two-dimensional SWE (2D-SWE), enabling real-time stiffness mapping under B-mode guidance.

Recent meta-analyses and prospective MASLD studies have demonstrated the high diagnostic accuracy of SWE for fibrosis staging, supporting its role as a complementary biomarker in comprehensive quantitative ultrasound protocols (51,52).

Despite its clinical utility, SWE remains susceptible to several confounding factors, including hepatic inflammation, cholestasis, postprandial state, elevated central venous pressure, and increased skin-to-capsule distance in obese individuals, all of which may lead to an overestimation of stiffness. Technical variability between vendors, probe frequency, and acquisition protocols further complicates cross-study comparability, emphasizing the need for standardized quality criteria and validated cut-off thresholds (51,53).

More recent developments include backscatter-based parameters and vendor-independent quantitative ultrasound techniques designed to improve standardization and reduce inter-

system variability. These approaches aim to decouple steatosis-related signal changes from confounding factors such as fibrosis, inflammation, and technical acquisition settings (54). Nevertheless, variability across ultrasound platforms and acquisition protocols remains a major challenge, emphasizing the importance of rigorous validation against established reference standards.

Phantom-based calibration and the use of MRI-PDFF as an external reference have been proposed as strategies to improve cross-vendor comparability and longitudinal consistency. Standardization efforts are particularly relevant for multicenter studies and for the integration of QUS into risk stratification models, where reproducibility and robustness are essential.

2.3 Rationale for a multiparametric imaging approach in MASLD

MASLD is characterized by biological complexity and spatial heterogeneity, with steatosis, inflammation, and fibrosis representing interconnected yet partially independent pathological processes. Quantification of hepatic fat alone provides limited prognostic information, as disease progression and clinical outcomes are more closely linked to fibrotic remodelling than to steatosis burden per se (19).

A uniparametric imaging approach fails to capture this complexity and may underestimate disease severity in patients with discordant pathological features. Conversely, multiparametric imaging aims to integrate complementary quantitative biomarkers, enabling a more comprehensive characterization of the liver's structural and functional state. In this context, quantitative ultrasound–based steatosis assessment, referenced to MRI-PDFF, can serve as a scalable component of broader imaging-based risk stratification frameworks that also incorporate elastography-derived stiffness and, where available, advanced MRI metrics such as iron quantification or inflammatory scores (55).

By combining parameters that reflect distinct biological processes, multiparametric imaging has the potential to improve patient stratification, identify individuals at increased risk of progression, and support personalized management strategies. This holistic assessment is crucial for identifying the "at-risk" MASH population (defined by the coexistence of MASH and advanced fibrosis), who would benefit most from intensive pharmacological intervention.

The integration of QUS into multiparametric imaging strategies has important clinical and translational implications. Given its accessibility, low cost, and suitability for

repeated measurements, QUS is particularly well suited for large-scale screening, longitudinal monitoring, and the assessment of therapeutic response in MASLD (56).

Anchoring ultrasound-derived metrics to MRI-PDFF enhances their interpretability and facilitates the harmonization of data across studies and clinical settings. This approach may reduce reliance on invasive procedures and enable broader implementation of imaging-based endpoints in both clinical practice and research. Ultimately, quantitative multiparametric imaging represents a key step toward precision medicine in MASLD, providing the foundation for risk-adapted surveillance and intervention strategies.

3. Research project

This chapter is based on the article “Performance of Ultrasound Liver Fat Quantification for the Assessment of Hepatic Steatosis Using MRI Fat Fraction as a Reference Standard” published in “Ultrasound in Medicine & Biology” of which I am a co-author and includes results previously published in the above-mentioned article (57).

3.1 Rationale and objectives

MASLD represents a highly prevalent and clinically heterogeneous condition, encompassing a wide spectrum of disease severity and outcomes. In this context, accurate and reproducible assessment of hepatic steatosis and fibrosis is of central importance, as these features are closely linked to disease progression, prognosis, and therapeutic decision-making. Although liver biopsy remains the reference standard for histological characterization, its invasiveness, associated risks, sampling variability, and limited acceptability severely restrict its applicability, particularly in a disease with such a high global prevalence.

Over the last decade, non-invasive imaging techniques have progressively assumed a pivotal role in the evaluation of MASLD. Magnetic resonance imaging–proton density fat fraction (MRI-PDFF) is currently regarded as the most accurate non-invasive method for quantifying hepatic fat content and serves as a reliable reference standard in both clinical research and therapeutic trials. However, its limited availability, higher costs, and longer examination times constrain its widespread use in routine clinical practice. Conversely, ultrasound-based techniques are widely accessible, cost-effective, and easily

repeatable, making them attractive tools for longitudinal monitoring, although their diagnostic performance has historically been variable and operator-dependent.

In this evolving landscape, quantitative ultrasound methods for liver fat assessment have emerged as promising alternatives to conventional qualitative approaches. Among these, liver fat quantification (LFQ) based on attenuation measurements has shown encouraging results, but comparative data against MRI-PDFF across different grades of steatosis and in heterogeneous patient populations remain limited.

The primary objective of this research project was therefore to perform a comprehensive quantitative multiparametric evaluation of hepatic steatosis in patients with known or suspected MASLD by directly comparing ultrasound-based LFQ with MRI-PDFF as the reference standard. Secondary objectives included the evaluation of the diagnostic performance of LFQ across increasing grades of steatosis, the assessment of its correlation with other ultrasound-derived parameters such as the HRI, and the investigation of its relationship with anthropometric and clinical variables. An additional exploratory objective was to assess liver stiffness using shear-wave elastography and to examine its association with the presence of cirrhosis, thereby providing a more integrated imaging-based characterization of MASLD.

3.2 Materials and methods

3.2.1 Study design

This investigation was designed as a single-center observational study conducted at a university hospital with dedicated expertise in liver imaging. Consecutive adult patients with known or suspected MASLD who were referred for imaging evaluation of liver disease were prospectively enrolled from May 2023 to December 2023. The observational design was chosen to reflect real-world clinical practice and to allow inclusion of patients with a broad range of disease severity, comorbidities, and underlying liver conditions.

The inclusion criteria were:

- patients over 18 years of age at the time of MRI examination.
- patients who have decided to participate in the study and have given informed consent after reading/listening and fully understanding the detailed explanations related to the clinical trial.
- patients with indication for an MRI study for either evaluation of liver pathology or characterization and follow-up of focal hepatic lesions.
- women not pregnant or breastfeeding.

All enrolled patients, who met the inclusion criteria and agreed to participate in this study, underwent both ultrasound and MRI examinations on the same day, minimizing the risk of temporal changes in hepatic fat content influencing comparative analyses. The study protocol was structured to enable direct head-to-head comparison between quantitative ultrasound-derived parameters and MRI-PDFF, while also allowing assessment of additional imaging markers related to liver stiffness and portal hypertension.

The following variables were recorded: age, sex, height, and weight for the calculation of body mass index (BMI, kg/m^2), underlying chronic liver disease and its etiology, and the presence of cirrhosis, as documented in the available clinical records.

3.2.2 Ultrasound imaging protocol

All ultrasound examinations were performed using the same ultrasound system (EPIQ Elite, software version 9.0.2; Philips Healthcare, Best, The Netherlands) equipped with a C5-1 transducer. Patients were examined in the supine position after a fasting period of at least six hours with their right arm extended above their heads. The right lobe of the liver was scanned by placing the ultrasound probe within the right intercostal space at the level of the middle axillary line. Image acquisition was performed while the patients held their breath to avoid motion artefacts.

The ultrasound protocol included:

- Measurement of the skin-to-liver capsule distance on the right hepatic lobe
- quantitative attenuation measurements for LFQ
- assessment of the hepatorenal index (HRI)
- liver stiffness measurement using two-dimensional shear-wave elastography (2D-SWE).

For LFQ assessment, attenuation measurements were obtained approximately 2 cm below the liver capsule, avoiding large vessels, focal lesions, and acoustic artifacts. A simultaneous color-coded confidence map and attenuation map were used to guide region-of-interest placement, with a predefined threshold of ≥ 60% to ensure measurement reliability. Ten measurements were acquired in different frames by placing a circular region of interest (ROI) measuring 3 cm in diameter, and the median value, IQR, and IQR-to-median ratio were recorded. The attenuation values were reported in dB/cm/MHz and measurements were considered reliable if the IQR/median ratio was below 30%.

Two operators with different levels of experience (a radiologist with 6 years of experience in ultrasound imaging and a senior radiology resident with 4 years of experience) performed the examinations to evaluate inter- and intra-operator reliability.

The hepatorenal index was calculated by placing a circular ROI of 1 cm of diameter in the liver and renal cortex at the same depth. As with LFQ, ten measurements were obtained, and reliability criteria were applied.

Liver stiffness measurements were performed using ElastQ Imaging, with a circular ROI of 1 cm of diameter positioned 1–2 cm below the liver capsule under confidence map guidance and the mean stiffness was recorded in kPa (Figure 5).

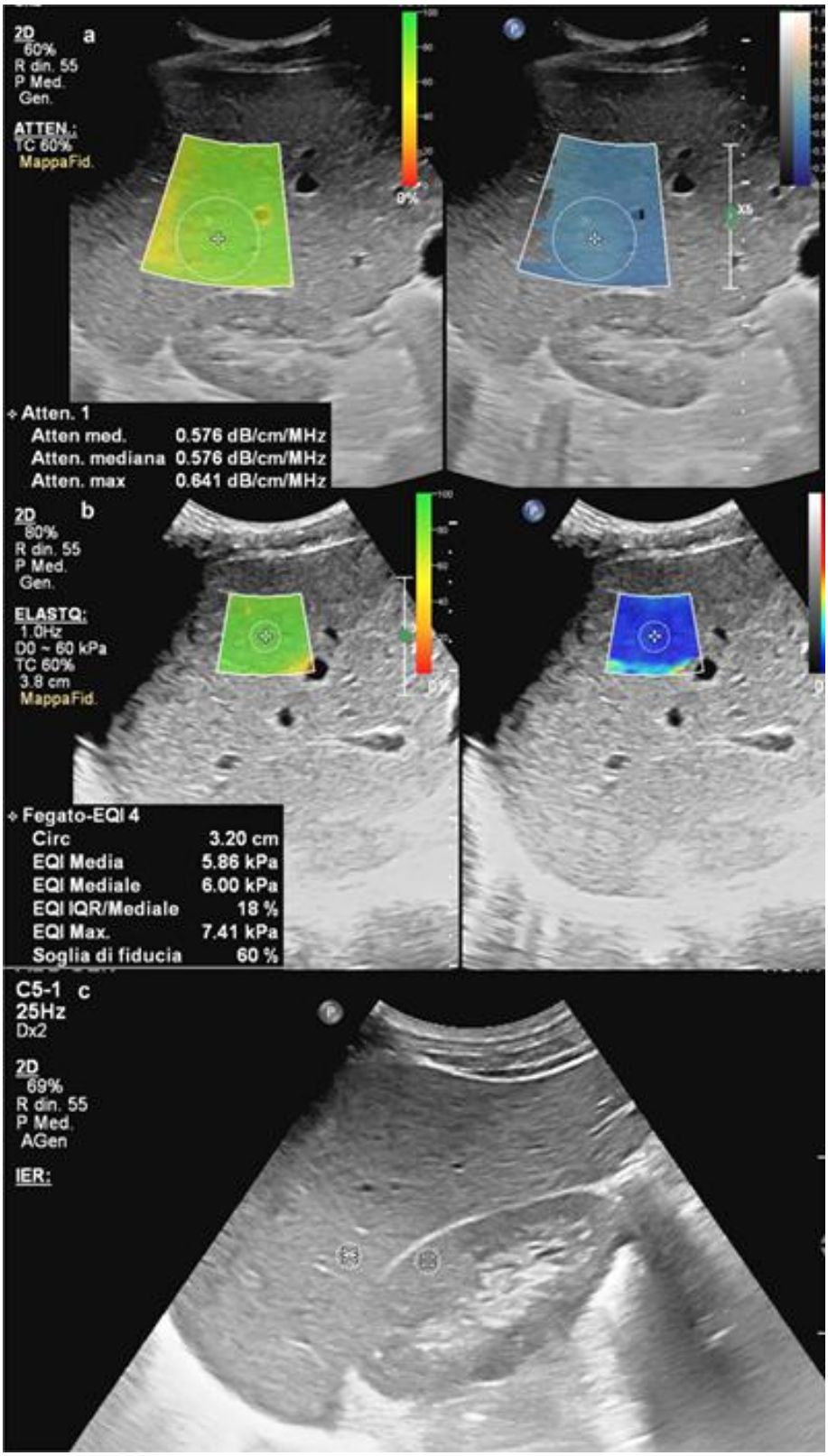

Figure 5 - Multi-parametric ultrasound examination of a 55-y.o. female including liver fat quantification (a), 2-D shear-wave elastography (b) and hepatorenal index (c) (57).

3.2.3 MRI protocol

All patients underwent MRI on a 3-T scanner (Philips Ingenia 3T) equipped with a 32-channel dStream anterior torso coil and using a standardized liver protocol. Hepatic steatosis was quantified using the mDixonQuant sequence, which provides proton density fat fraction maps (Table 1).

Table 1: Acquisition parameters of mDIXONQuant sequence.

Parameters	mDIXONQuant
Image plane	Axial
TR (ms)	5.6
First TE (ms)/delta TE	0.97/0.7
Number of echoes	6
Flip Angle (degrees)	3
Number of slices	84
Slice Thickness (mm)	6
Reconstruction Interval (mm)	0
Acquisition Matrix	176x151
Field of View (mm)	RL:440; AP:377; FH:252
Number of Excitations	1
Acquisition time (s)	18

TE: Time of Echo; TR: Repetition Time.

Circular regions of interest measuring 2–3 cm^2 were placed in multiple liver segments, avoiding vessels and focal lesions, and the median fat fraction was recorded as the reference standard.

Based on established thresholds, patients were classified as having no steatosis (<5.1%), grade 1 steatosis (5.1–14.4%), grade 2 steatosis (14.5–20.6%), or grade 3 steatosis (>20.6%) (58). Additional MRI findings, including splenic length, presence of ascites, and porto-systemic collaterals, were also recorded.

3.2.4 Outcomes

The primary outcome was the diagnostic performance of LFQ for the detection and grading of hepatic steatosis, using MRI-PDFF as the reference standard. Secondary outcomes included the correlation of LFQ with MRI fat fraction, HRI, BMI, and skin-to-liver capsule distance, as well as the comparison of LFQ performance in patients with and without cirrhosis. Additional outcomes involved the diagnostic performance of HRI and the ability of shear-wave elastography to identify cirrhosis.

3.2.5 Statistical analysis

Categorical variables were reported as numbers and percentages, and they were compared using the Pearson $\chi 2$ or Fisher's exact test. Continuous variables were provided with a median with 25th to 75th percentiles after testing for normality with the Shapiro-Wilk test (with a significance level of $p < 0.05$ indicating that the data do not follow a normal distribution). A Kruskal-Wallis test was used to compare differences in continuous variables among steatosis grades, while a Mann-Whitney U test was used for pair-wise comparisons. The intra- and inter-operator reliability of LFQ measurements was evaluated using the intra-class correlation coefficient (ICC) with 95% confidence intervals (CIs), with absolute agreement with the two-way mixed effects model. Agreement was defined as poor (ICC 0.90) (59). Spearman's rank order correlation (Spearman's ρ) was calculated between LFQ, HRI, MRI fat fraction and BMI.

Diagnostic performance was evaluated using the area under the receiver operator characteristic curve (AUC) and its 95% CI for each steatosis grade. Optimal cutoffs and their sensitivity and specificity were determined based on the Youden index. The AUCs of LFQ and HRI were compared using a DeLong test in the subset of patients with both reliable measurements. The statistical significance level was set at $p < 0.05$. Statistical analysis was performed using IBM SPSS software version 26.0 (IBM Corp, Armonk, NY, USA) and MedCalc Statistical Software version 14.8.1 (Ostend, Belgium).

3.3 Results

3.3.1 Study population

The study population consisted of 152 patients with a median age of 64.0 years (interquartile range [IQR] 52.3–78.7 years). The cohort included 77 males (50.7%) and 75 females (49.3%). The median MRI fat fraction was 4.5%. According to the MRI reference standard, 92 (60.5%) patients were classified as having no steatosis, 39 (25.7%) had grade 1, and 11 (7.2%) had grade 2, and 10 (6.6%) had grade 3 steatosis.

The median BMI was 25.7 kg/m² (IQR 23.4–29.4 kg/m²), with a statistically significant increase in BMI across steatosis grades. Forty-eight patients (31.6%) were classified as overweight and 35 (23.0%) as obese. Based on the calculated BMI, participants were categorized according to World Health Organization standard thresholds as underweight (BMI < 18.5 kg/m^2), normal weight (BMI 18.5 to < 25 kg/m^2), overweight (BMI 25 to < 30 kg/m^2) or obese (BMI ≥ 30 kg/m^2) (60).

A history of chronic liver disease was present in 56 patients (36.8%), with hepatitis C virus infection representing the most common etiology. MASLD was significantly more frequent among patients with MRI-detected hepatic steatosis compared with those without steatosis. Cirrhosis was present in 43 patients (28.3%), with imaging evidence of ascites and porto-systemic collaterals observed in a subset of cases. Significant differences among steatosis grades were also observed for splenic length and skin-to-liver capsule distance (Table 2).

Table 2 – Clinical characteristics of the included participants, with a comparison among steatosis grades (57).

	Total (n = 152)	No steatosis (n = 92)	Steatosis grade 1 (n = 39)	Steatosis grade 2 (n = 11)	Steatosis grade 3 (n = 10)	p value
Age (years)	64.0 (52.3-78.7)	66.0 (50.8-74.0)	59.0 (50.0-69.3)	61.0 (55.0-70.0)	64.0 (56.5-65.5)	0.523
Sex						0.320
Males	77 (50.7)	46 (50.0)	23 (59.0)	3 (27.3)	5 (50.0)	
Females	75 (49.3)	46 (50.0)	16 (41.0)	8 (72.7)	5 (50.0)	
BMI (kg/m^2)	25.7 (23.4-29.4)	24.4 (21.8-26.7)	26.7 (24.6-31.1)	31.6 (28.2-40.9)	29.4 (26.6-32.9)	**< 0.001**
BMI classification						**< 0.001**
Underweight	6 (3.9)	6 (6.5)	0 (0)	0 (0)	0 (0)	
Normal weight	63 (41.4)	49 (53.3)	12 (30.8)	0 (0)	2 (20.0)	
Overweight	48 (31.6)	12 (30.8)	12 (30.8)	4 (36.4)	3 (30.0)	
Obesity	35 (23.0)	8 (8.7)	15 (38.5)	7 (63.6)	5 (50.0)	
Chronic liver disease						
Hepatitis C	17 (11.2)	14 (15.2)	2 (5.1)	0 (0)	1 (10.0)	0.226
Hepatitis B	7 (4.3)	4 (4.3)	2 (5.1)	0 (0)	0 (0)	0.745
MASLD	14 (9.2)	3 (3.3)	8 (20.5)	1 (9.1)	2 (20.0)	**0.010**
Alcohol	4 (2.6)	3 (3.3)	0 (0)	0 (0)	1 (10.0)	0.306
Other	14 (9.2)	6 (6.5)	7 (17.9)	1 (9.1)	1 (10.0)	0.147
None	96 (63.2)	62 (64.4)	20 (51.3)	9 (81.8)	5 (50.0)	0.141
Cirrhosis	43 (28.3)	24 (26.1)	14 (35.9)	2 (18.2)	3 (30.0)	0.593
Ascites	6 (3.9)	6 (6.4)	0 (0)	0 (0)	0 (0)	0.254
Abdominal varices	22 (14.5)	13 (14.1)	7 (17.9)	1 (9.1)	1 (10.0)	0.847
MRI fat fraction	4.5 (3.3-7.9)	3.6 (2.7-4.3)	7.2 (6.3-9.1)	16.6 (15.2-18.0)	22.7 (21.3-25.4)	**< 0.001**
Spleen length (cm)	10.7 (9.5-12.7)	10.4 (9.3-12.2)	11.7 (10.2-14.0)	11.1 (9.9-12.3)	12.0 (11.1-13.5)	**0.013**
Skin-to-liver capsule distance (cm)	1.8 (1.4-2.2)	1.7 (1.3-2.0)	2.0 (1.6-2.3)	2.5 (2.2-3.3)	2.3 (1.7-2.6)	**< 0.001**

Continuous variables are provided as medians with 25th to 75th percentiles in parenthesis, categorical variables are provided as numbers and percentages in parenthesis. Statistically significant values ($p<0.05$) are provided in bold. BMI, body mass index; MASLD, metabolic dysfunction-associated steatotic liver disease; MRI, magnetic resonance imaging.

3.3.2 Liver fat quantification

LFQ measurements (Table 3) were successfully obtained in all patients, with a 100% success rate and a median IQR/median ratio of 2.0%. The median LFQ was 0.58 dB/cm/MHz (range 0.42−0.84 dB/cm/MHz) and LFQ values differed significantly across steatosis grades, with progressively higher attenuation measurements observed with increasing steatosis severity (Figures 6, 7).

Table 3 – Median liver fat quantification values, hepatorenal index and liver stiffness measurement with their interquartile range and IQR/Med (%) according to steatosis grade (57).

	Total (*n* = 152)	No steatosis (*n* = 92)	Steatosis grade 1 (*n* = 39)	Steatosis grade 2 (*n* = 11)	Steatosis grade 3 (*n* = 10)	*p* value
LFQ (dB/cm/MHz)	0.58 (0.54-0.65)	0.56 (0.52-0.58)	0.64 (0.60-0.67)	0.70 (0.65-0.75)	0.73 (0.71-0.77)	**< 0.001**
IQR (dB/cm/MHz)	0.01 (0.01-0.02)	0.01 (0.01-0.02)	0.01 (0.01-0.02)	0.01 (0.01-0.02)	0.01 (0.01-0.02)	0.661
IQR/Med (%)	2.0 (1.3-3.0)	2.0 (2.0-4.0)	2.0 (1.0-3.0)	1.0 (1.0-3.0)	1.0 (0.8-3.0)	**0.008**
HRI*	1.21 (0.85-1.70)	1.00 (0.79-1.38)	1.38 (0.93-1.99)	1.98 (1.10-2.42)	1.97 (1.67-2.95)	**< 0.001**
IQR	0.13 (0.09-0.24)	0.11 (0.07-0.20)	0.15 (0.09-0.29)	0.14 (0.10-0.27)	0.27 (0.18-0.35)	**0.001**
IQR/Med (%)	12.0 (8.0-17.0)	13.0 (7.0-18.0)	12.0 (8.0-20.0)	10.5 (6.0-12.0)	11.0 (8.5-16.0)	0.890
LSM (kPa)	5.75 (4.75-9.53)	5.69 (4.66-7.76)	5.65 (4.58-10.50)	6.10 (4.81-10.05)	9.38 (5.77-14.45)	0.141
IQR (kPa)	0.30 (0.16-0.77)	0.25 (0.16-0.56)	0.35 (0.10-0.81)	0.80 (0.20-1.10)	0.40 (0.20-0.65)	0.538

Continuous variables are provided as medians with 25th to 75th percentiles in parenthesis. Statistically significant values ($p < 0.05$) are provided in bold. LFQ values are provided according to the values registered by the first radiologist measurements. HRI, hepatorenal index; IQR, interquartile range; LFQ, liver fat quantification; LSM, liver stiffness measurement; Med, median.

* HRI values are provided for the 131 patients with valid measurements (IQR/Med < 30%), including 79 patients with no steatosis, 35 with grade 1, 8 with grade 2, and 9 with grade 3 steatosis.

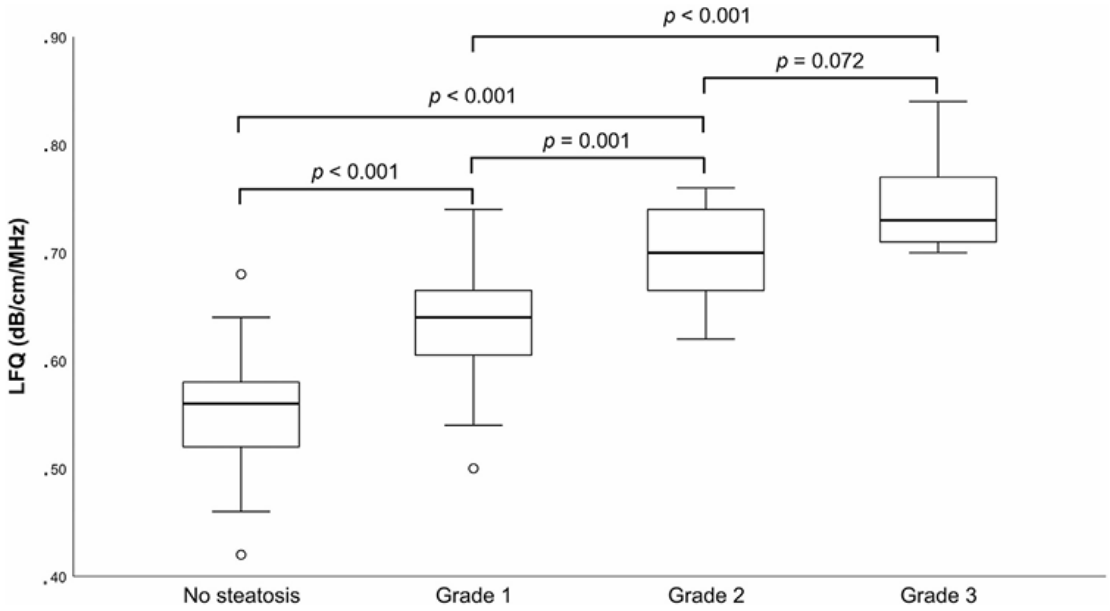

Figure 6 - Plot box graph showing pair-wise comparison of liver fat quantification (LFQ) measurements between steatosis grades (57).

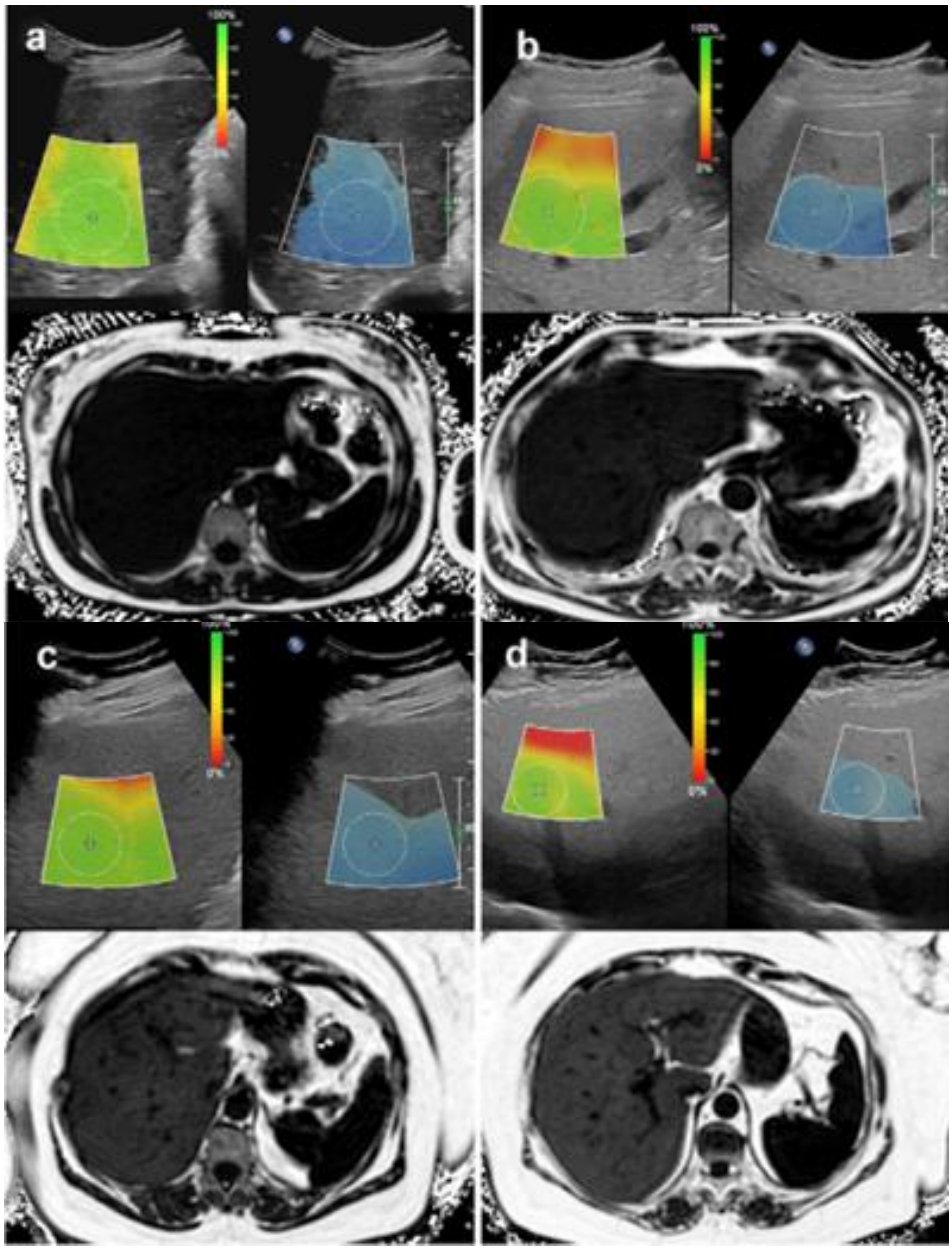

Figure 7 – LFQ with corresponding magnetic resonance imaging fat fraction maps. (a) A 75-y.o. female with a median LFQ of 0.57 dB/ cm/MHz and fat fraction of 3.9%, consistent with the absence of steatosis. (b) A 63-y.o. male with a median LFQ of 0.61 dB/cm/MHz and fat fraction of 6.8%, consistent with grade 1 steatosis. (c) A 56-year-old female with a median LFQ of 0.68 dB/cm/MHz and fat fraction of 16.7%, consistent with grade 2 steatosis. (d) A 23-y.o. female with a median LFQ of 0.73 dB/cm/MHz and fat fraction of 21.4%, consistent with grade 3 steatosis (57).

LFQ demonstrated a strong correlation with MRI fat fraction ($\rho = 0.715$; $p < 0.001$), a moderate correlation with HRI ($\rho = 0.448$; $p < 0.001$), and weaker but significant correlations with BMI ($\rho = 0.355$; $p < 0.001$) and skin-to-liver capsule distance ($\rho = 0.259$; $p = 0.001$).

LFQ showed excellent diagnostic performance for the detection of steatosis, with an AUC of 0.919 for grade ≥1, 0.970 for grade ≥2, and 0.974 for grade 3 steatosis (Table 4).

Cutoff values were determined according to the Youden index and were set:

- > 0.60 dB/cm/MHz for grade ≥1 (sensitivity 80.3%; specificity 92.4%).
- > 0.64 dB/cm/MHz for grade ≥2 (sensitivity 95.2%; specificity 85.5%).
- > 0.69 dB/cm/MHz for grade 3 (sensitivity 100%; specificity 93.7%).

Table 4 – Performance of liver fat quantification and hepatorenal index for the diagnosis of steatosis grades with sensitivity and specificity according to the optimal cutoffs (57).

	Prevalence	AUC (95% CI)	*p* value	Cutoff	Se (95% CI)	Sp (95% CI)
LFQ						
Grade ≥1	60	0.919 (0.861-0.956)	< 0.001	> 0.60	80.3 (71.5-91.7)	92.4 (84.9-96.6)
Grade ≥2	21	0.970 (0.929-0.991)	< 0.001	> 0.64	95.2 (76.2-99.9)	85.5 (78.3-91.0)
Grade 3	10	0.974 (0.935-0.993)	< 0.001	> 0.69	100 (69.2-100)	93.7 (88.3-97.1)
HRI						
Grade ≥1	52	0.724 (0.640-0.799)	< 0.001	> 1.33	65.4 (50.9-78.0)	74.7 (63.6-83.8)
Grade ≥2	17	0.812 (0.735-0.875)	< 0.001	> 1.55	82.4 (56.6-96.2)	78.1 (69.4-85.3)
Grade 3	9	0.847 (0.773-0.904)	< 0.001	> 1.65	88.9 (51.8-99.7)	77.1 (68.6-84.2)

Cutoff values were determined according to the Youden index, and they are provided in dB/cm/MHz for ultrasound-guided attenuation parameter. AUC, area under the receiver operator characteristic curve; HRI, hepatorenal index; LFQ, liver fat quantification; Se, sensitivity; Sp, specificity.

* HRI values are provided for the 131 patients with valid measurements (IQR/Med<30%).

The intra- and inter-operator reliability of LFQ measurements was good, with an ICC of 0.88 (95% CI: 0.83−0.91) and 0.85 (95% CI: 0.79 −0.89), respectively.

Diagnostic performance was slightly reduced in patients with cirrhosis and in patients with a skin-to-liver capsule distance < 1.8 cm but remained statistically significant. There are no variations in diagnostic performance according to BMI (Table 5).

Table 5 – diagnostic performance for diagnosis of steatosis (57).

Patients	AUC (95% CI)	*p* value
with cirrhosis	0.865 (0.726-0.950)	< 0.001
without cirrhosis	0.938 (0.876-0.976)	< 0.001
with a skin-to-liver capsule distance < 1.8 cm	0.891 (0.795-0.988)	< 0.001
with a skin-to-liver capsule distance ≥ 1.8 cm	0.937 (0.882-0.991)	< 0.001
with BMI < 25 kg/m^2	0.918 (0.826-1.000)	< 0.001
with BMI ≥ 25 kg/m^2	0.910 (0.845-0.976)	< 0.001

3.3.3 Hepatorenal index

HRI demonstrated an 86.2% success rate due to:

- IQR/Med ≥ 30% (9.2%)
- prior right nephrectomy (2%)
- dysmorphic hepatic lobe (2%)
- polycystic kidney disease (0.6%).

The median HRI was 1.21, with a significant difference among steatosis grades (p <0.001) (Figure 8), despite HRI showed lower diagnostic accuracy than LFQ across all steatosis grades (Figure 9).

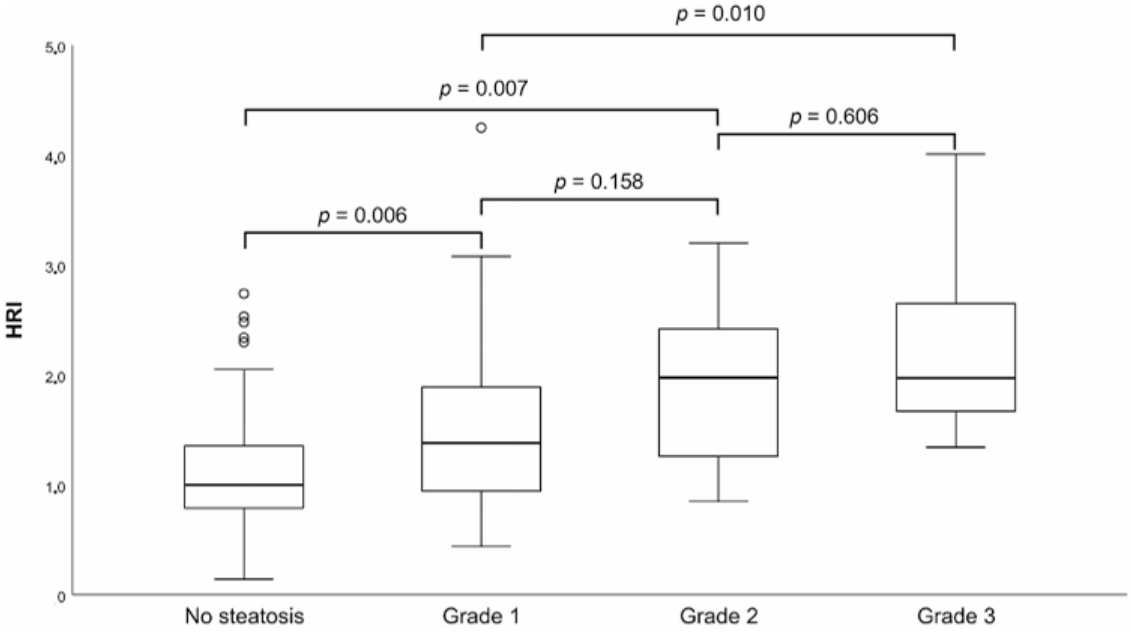

Figure 8 – Plot box graph with pair-wise comparison of hepatorenal index (HRI) measurements between steatosis grades (57).

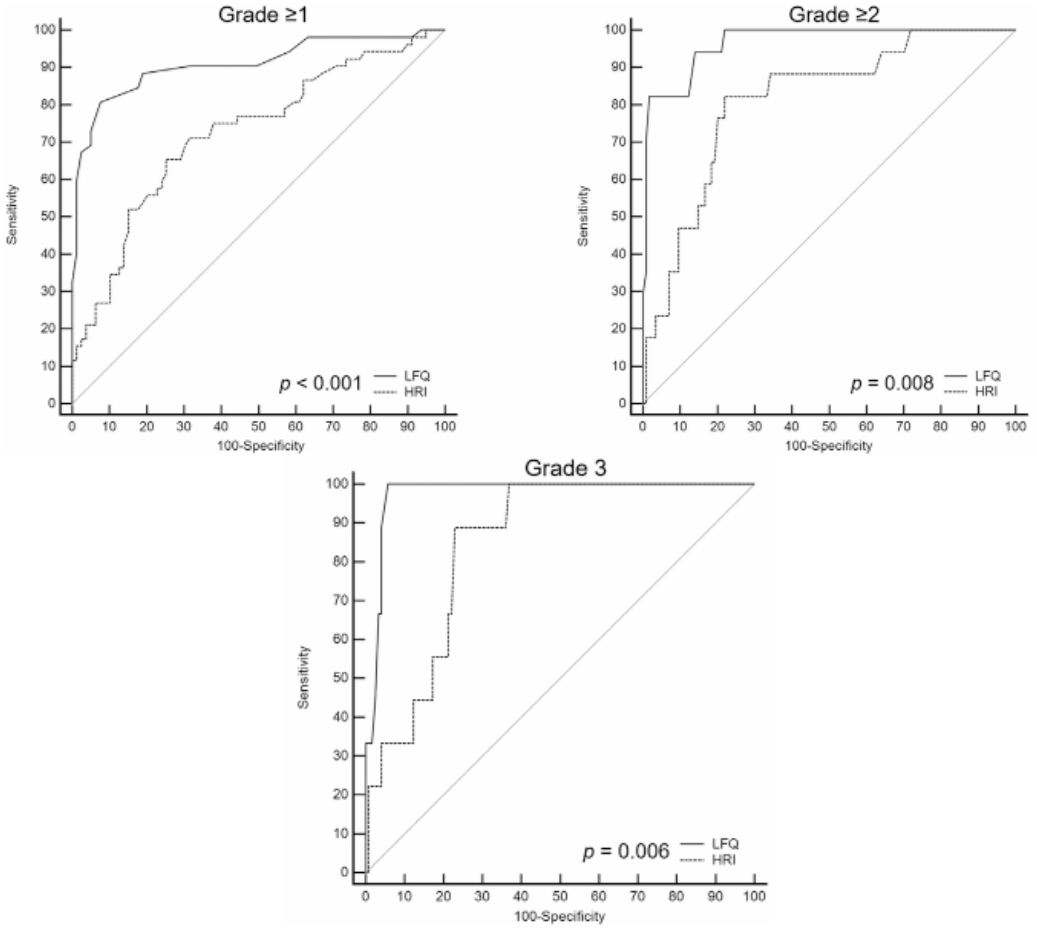

Figure 9 – Comparison of receiver operator characteristic curves of LFQ and the HRI for the diagnosis of steatosis grades (57).

3.3.4 Shear-wave elastography

Shear-wave elastography did not show significant differences across steatosis grades but demonstrated excellent performance for the identification of cirrhosis, with an AUC of 0.931 (95% CI: 0.878−0.966, p < 0.001) with an optimal cutoff of > 6.31 kPa providing high sensitivity (95.4%; 95% CI: 84.2−99.4%) and good specificity (80.7%; 95% CI: 72.1−87.7%).

3.4 Discussion

The present study provides a comprehensive evaluation of quantitative ultrasound-based liver fat quantification within a heterogeneous cohort of patients with MASLD, using MRI-PDFF as a non-invasive reference standard (3,4).

The findings demonstrate that LFQ achieves high diagnostic accuracy across increasing grades of steatosis, with strong correlation with MRI-derived fat fraction and clear discrimination between steatosis categories. LFQ measurements also demonstrated good inter- and intra-operator reliability. These results support and extend previous evidence indicating that attenuation-based ultrasound techniques can overcome several of the limitations historically associated with conventional qualitative ultrasound assessment (61).

The strong correlation observed between LFQ and MRI-PDFF is consistent with prior studies reporting robust agreement between quantitative ultrasound attenuation parameters and MRI-based fat quantification (62,63).

MRI-PDFF is widely regarded as the most accurate non-invasive method for assessing hepatic steatosis, owing to its ability to sample the entire liver parenchyma and correct for confounding factors such as T1 bias and iron overload (64,65). In this context, the close alignment between LFQ and MRI-PDFF observed in the present study supports the validity of LFQ as a reliable surrogate for hepatic fat quantification, particularly in clinical scenarios where MRI availability is limited or repeated assessments are required.

Importantly, LFQ demonstrated superior feasibility and diagnostic performance compared with the HRI. While HRI has historically been used as a semi-quantitative

ultrasound marker of steatosis, its applicability is limited by anatomical constraints, operator dependence, and reduced reliability in patients with renal abnormalities or advanced liver disease (66,67). In the present cohort, HRI could not be reliably obtained in a non-negligible proportion of patients, and its diagnostic accuracy was consistently inferior to that of LFQ across all steatosis grades. These findings are in line with previous reports questioning the robustness of ratio-based ultrasound metrics and further support a transition toward fully quantitative ultrasound approaches (68,69).

A clinically relevant aspect of this study is the evaluation of LFQ performance in patients with cirrhosis. Advanced liver disease is known to alter hepatic architecture and acoustic properties, potentially confounding fat quantification (70). Although a modest reduction in diagnostic accuracy was observed in cirrhotic patients, LFQ maintained good performance even in this challenging subgroup.

The analysis of shear-wave elastography findings further highlights the complementary nature of multiparametric ultrasound assessment. As expected, liver stiffness measurements did not differ significantly across steatosis grades, confirming that stiffness primarily reflects fibrotic remodelling rather than fat accumulation (71). However, shear-wave elastography demonstrated excellent accuracy for the identification of cirrhosis, reinforcing its role as a prognostic marker. The combined use of LFQ for steatosis quantification and elastography for fibrosis assessment enables comprehensive, non-invasive liver phenotyping within a single imaging session.

From a clinical perspective, the integration of quantitative ultrasound techniques into routine practice has important implications for the management of MASLD. Given the high prevalence of the disease and the limited availability of MRI in many healthcare

settings, scalable and cost-effective tools for steatosis assessment are urgently needed. Ultrasound-based LFQ offers a practical solution that may facilitate early detection of hepatic steatosis, support risk stratification, and enable longitudinal monitoring of disease progression or therapeutic response.

Moreover, the ability to combine LFQ and elastography during a single ultrasound examination aligns with current recommendations advocating stepwise, noninvasive assessment strategies for MASLD. Such an approach may reduce unnecessary referrals for invasive procedures, optimize resource utilization, and improve patient adherence to follow-up protocols.

The present study has several notable strengths.

First, it adopts a multiparametric imaging approach that integrates quantitative ultrasound techniques with MRI-PDFF, allowing a robust head-to-head comparison between a widely accessible modality and a validated non-invasive reference standard.

Second, the inclusion of a relatively large and heterogeneous patient cohort, encompassing different grades of steatosis and a substantial proportion of cirrhotic patients, enhances the clinical relevance and generalizability of the findings.

Third, the standardized imaging protocols, the use of predefined quality criteria for measurement reliability, and the assessment of inter- and intra-operator reproducibility strengthen the methodological rigor of the study. Finally, the evaluation of multiple ultrasound-derived parameters within the same population provides a comprehensive overview of their relative diagnostic performance in MASLD.

Several limitations should also be acknowledged. The number of patients with moderate to severe steatosis was relatively limited, which may have affected the precision of cutoff estimates for higher steatosis grades. Histopathological correlation was not available, and MRI-PDFF was used as the reference standard; although MRI-PDFF is widely accepted as the most accurate non-invasive technique for fat quantification, it does not provide direct information on necroinflammatory activity. In addition, controlled attenuation parameter measurements were not included, precluding a direct comparison with other elastography-based attenuation techniques. Finally, the single-center design may limit external validity, and longitudinal data were not available to assess changes over time or response to therapeutic interventions. Multicentre studies with larger numbers of patients with moderate-to-severe steatosis will be essential to refine cutoff values and confirm generalizability across different ultrasound platforms and clinical settings.

3.5 Conclusions

This study supports the role of multiparametric quantitative imaging as a robust, feasible, and clinically meaningful tool for the assessment of hepatic steatosis in MASLD. When combined with shear-wave elastography, LFQ enables a comprehensive, non-invasive evaluation of both steatosis and fibrosis, aligning with modern paradigms of personalized and multiparametric liver imaging. These findings provide a strong rationale for the incorporation of quantitative ultrasound techniques into routine MASLD assessment and for their further evaluation in longitudinal and interventional studies.

4. References

1. Younossi ZM, Golabi P, Paik JM, Henry A, Van Dongen C, Henry L. The global epidemiology of nonalcoholic fatty liver disease (NAFLD) and nonalcoholic steatohepatitis (NASH): a systematic review. Hepatology. aprile 2023;77(4):1335–47. doi:10.1097/HEP.0000000000000004

2. Younossi ZM, Golabi P, Price JK, Owrangi S, Gundu-Rao N, Satchi R, et al. The Global Epidemiology of Nonalcoholic Fatty Liver Disease and Nonalcoholic Steatohepatitis Among Patients With Type 2 Diabetes. Clinical Gastroenterology and Hepatology. ottobre 2024;22(10):1999-2010.e8. doi:10.1016/j.cgh.2024.03.006

3. Diaz Torres JV, Villanueva Guerrero VR, Vargas Gómez JP, Pacheco Miranda FJ, Orozco Álvarez LR, León Insignares JD, et al. Metabolic Dysfunction Associated to Steatotic Liver Disease: A Review. Metabolic Syndrome and Related Disorders. dicembre 2025;23(10):427–39. doi:10.1177/15578518251382048

4. Tilg H, Petta S, Stefan N, Targher G. Metabolic Dysfunction–Associated Steatotic Liver Disease in Adults: A Review. JAMA. 13 gennaio 2026;335(2):163. doi:10.1001/jama.2025.19615

5. Chalasani N, Younossi Z, Lavine JE, Charlton M, Cusi K, Rinella M, et al. The diagnosis and management of nonalcoholic fatty liver disease: Practice guidance from the American Association for the Study of Liver Diseases. Hepatology. gennaio 2018;67(1):328–57. doi:10.1002/hep.29367

6. Tacke F, Horn P, Wai-Sun Wong V, Ratziu V, Bugianesi E, Francque S, et al. EASL–EASD–EASO Clinical Practice Guidelines on the management of metabolic dysfunction-associated

steatotic liver disease (MASLD). Journal of Hepatology. settembre 2024;81(3):492–542. doi:10.1016/j.jhep.2024.04.031

7. Friedman SL, Neuschwander-Tetri BA, Rinella M, Sanyal AJ. Mechanisms of NAFLD development and therapeutic strategies. Nat Med. luglio 2018;24(7):908–22. doi:10.1038/s41591-018-0104-9

8. Tilg H, Moschen AR. Evolution of Inflammation in Nonalcoholic Fatty Liver Disease: The Multiple Parallel Hits Hypothesis. Hepatology. novembre 2010;52(5):1836–46. doi:10.1002/hep.24001

9. Buzzetti E, Pinzani M, Tsochatzis EA. The multiple-hit pathogenesis of non-alcoholic fatty liver disease (NAFLD). Metabolism. agosto 2016;65(8):1038–48. doi:10.1016/j.metabol.2015.12.012

10. Schnabl B, Damman CJ, Carr RM. Metabolic dysfunction–associated steatotic liver disease and the gut microbiome: pathogenic insights and therapeutic innovations. Journal of Clinical Investigation. 1 aprile 2025;135(7):e186423. doi:10.1172/JCI186423

11. Romeo S, Kozlitina J, Xing C, Pertsemlidis A, Cox D, Pennacchio LA, et al. Genetic variation in PNPLA3 confers susceptibility to nonalcoholic fatty liver disease. Nat Genet. dicembre 2008;40(12):1461–5. doi:10.1038/ng.257

12. Boursier J, Diehl AM. Nonalcoholic Fatty Liver Disease and the Gut Microbiome. Clinics in Liver Disease. maggio 2016;20(2):263–75. doi:10.1016/j.cld.2015.10.012

13. Mofrad P, Contos MJ, Haque M, Sargeant C, Fisher RA, Luketic VA, et al. Clinical and Histologic Spectrum of Nonalcoholic Fatty Liver Disease Associated With Normal Alt Values. Hepatology. giugno 2003;37(6):1286–92. doi:10.1053/jhep.2003.50229

14. Eslam M, Newsome PN, Sarin SK, Anstee QM, Targher G, Romero-Gomez M, et al. A new definition for metabolic dysfunction-associated fatty liver disease: An international expert consensus statement. Journal of Hepatology. luglio 2020;73(1):202–9. doi:10.1016/j.jhep.2020.03.039

15. Rinella ME, Lazarus JV, Ratziu V, Francque SM, Sanyal AJ, Kanwal F, et al. A multisociety Delphi consensus statement on new fatty liver disease nomenclature. Hepatology. dicembre 2023;78(6):1966–86. doi:10.1097/HEP.0000000000000520

16. Cusi K, Abdelmalek MF, Apovian CM, Balapattabi K, Bannuru RR, Barb D, et al. Metabolic Dysfunction–Associated Steatotic Liver Disease (MASLD) in People With Diabetes: The Need for Screening and Early Intervention. A Consensus Report of the American Diabetes Association. Diabetes Care. 1 luglio 2025;48(7):1057–82. doi:10.2337/dci24-0094

17. Lonardo A, Nascimbeni F, Ballestri S, Fairweather D, Win S, Than TA, et al. Sex Differences in Nonalcoholic Fatty Liver Disease: State of the Art and Identification of Research Gaps. Hepatology. ottobre 2019;70(4):1457–69. doi:10.1002/hep.30626

18. Miller DM, McCauley KF, Dunham-Snary KJ. Metabolic Dysfunction-Associated Steatotic Liver Disease (MASLD): Mechanisms, Clinical Implications and Therapeutic Advances. Endocrino Diabet & Metabol. novembre 2025;8(6):e70132. doi:10.1002/edm2.70132

19. Angulo P, Kleiner DE, Dam-Larsen S, Adams LA, Bjornsson ES, Charatcharoenwitthaya P, et al. Liver Fibrosis, but No Other Histologic Features, Is Associated With Long-term Outcomes of Patients With Nonalcoholic Fatty Liver Disease. Gastroenterology. agosto 2015;149(2):389-397.e10. doi:10.1053/j.gastro.2015.04.043

20. Singh S, Allen AM, Wang Z, Prokop LJ, Murad MH, Loomba R. Fibrosis Progression in Nonalcoholic Fatty Liver vs Nonalcoholic Steatohepatitis: A Systematic Review and Meta-analysis of Paired-Biopsy Studies. Clinical Gastroenterology and Hepatology. aprile 2015;13(4):643-654.e9. doi:10.1016/j.cgh.2014.04.014

21. Dulai PS, Singh S, Patel J, Soni M, Prokop LJ, Younossi Z, et al. Increased risk of mortality by fibrosis stage in nonalcoholic fatty liver disease: Systematic review and meta-analysis. Hepatology. maggio 2017;65(5):1557–65. doi:10.1002/hep.29085

22. Loomba R, Friedman SL, Shulman GI. Mechanisms and disease consequences of nonalcoholic fatty liver disease. Cell. maggio 2021;184(10):2537–64. doi:10.1016/j.cell.2021.04.015

23. Trefts E, Gannon M, Wasserman DH. The liver. Current Biology. novembre 2017;27(21):R1147–51. doi:10.1016/j.cub.2017.09.019

24. Kietzmann T. Metabolic zonation of the liver: The oxygen gradient revisited. Redox Biology. aprile 2017;11:622–30. doi:10.1016/j.redox.2017.01.012

25. Ben-Moshe S, Itzkovitz S. Spatial heterogeneity in the mammalian liver. Nat Rev Gastroenterol Hepatol. luglio 2019;16(7):395–410. doi:10.1038/s41575-019-0134-x

26. Ferré P, Phan F, Foufelle F. SREBP-1c and lipogenesis in the liver: an update. Biochemical Journal. 29 ottobre 2021;478(20):3723–39. doi:10.1042/BCJ20210071

27. Todisco S, Santarsiero A, Convertini P, De Stefano G, Gilio M, Iacobazzi V, et al. PPAR Alpha as a Metabolic Modulator of the Liver: Role in the Pathogenesis of Nonalcoholic Steatohepatitis (NASH). Biology. 23 maggio 2022;11(5):792. doi:10.3390/biology11050792

28. Donnelly KL, Smith CI, Schwarzenberg SJ, Jessurun J, Boldt MD, Parks EJ. Sources of fatty acids stored in liver and secreted via lipoproteins in patients with nonalcoholic fatty liver disease. J Clin Invest. 2 maggio 2005;115(5):1343–51. doi:10.1172/JCI23621

29. Lambert JE, Ramos–Roman MA, Browning JD, Parks EJ. Increased De Novo Lipogenesis Is a Distinct Characteristic of Individuals With Nonalcoholic Fatty Liver Disease. Gastroenterology. marzo 2014;146(3):726–35. doi:10.1053/j.gastro.2013.11.049

30. Finelli C. Molecular Mechanisms and Mediators of Hepatotoxicity Resulting from an Excess of Lipids and Non-Alcoholic Fatty Liver Disease. Gastrointestinal Disorders. 25 maggio 2023;5(2):243–60. doi:10.3390/gidisord5020020

31. Kuchay MS, Choudhary NS, Ramos-Molina B. Pathophysiological underpinnings of metabolic dysfunction-associated steatotic liver disease. American Journal of Physiology-Cell Physiology. 1 maggio 2025;328(5):C1637–66. doi:10.1152/ajpcell.00951.2024

32. Vilar-Gomez E, Martinez-Perez Y, Calzadilla-Bertot L, Torres-Gonzalez A, Gra-Oramas B, Gonzalez-Fabian L, et al. Weight Loss Through Lifestyle Modification Significantly Reduces Features of Nonalcoholic Steatohepatitis. Gastroenterology. agosto 2015;149(2):367-378.e5. doi:10.1053/j.gastro.2015.04.005

33. Loomba R, Hartman ML, Lawitz EJ, Vuppalanchi R, Boursier J, Bugianesi E, et al. Tirzepatide for Metabolic Dysfunction–Associated Steatohepatitis with Liver Fibrosis. N Engl J Med. 25 luglio 2024;391(4):299–310. doi:10.1056/NEJMoa2401943

34. Harrison SA, Bedossa P, Guy CD, Schattenberg JM, Loomba R, Taub R, et al. A Phase 3, Randomized, Controlled Trial of Resmetirom in NASH with Liver Fibrosis. N Engl J Med. 8 febbraio 2024;390(6):497–509. doi:10.1056/NEJMoa2309000

35. Lassailly G, Caiazzo R, Ntandja-Wandji LC, Gnemmi V, Baud G, Verkindt H, et al. Bariatric Surgery Provides Long-term Resolution of Nonalcoholic Steatohepatitis and Regression of Fibrosis. Gastroenterology. ottobre 2020;159(4):1290-1301.e5. doi:10.1053/j.gastro.2020.06.006

36. Stefan N, Häring HU, Cusi K. Non-alcoholic fatty liver disease: causes, diagnosis, cardiometabolic consequences, and treatment strategies. The Lancet Diabetes & Endocrinology. aprile 2019;7(4):313–24. doi:10.1016/S2213-8587(18)30154-2

37. Noureddin M, Lam J, Peterson MR, Middleton M, Hamilton G, Le TA, et al. Utility of magnetic resonance imaging versus histology for quantifying changes in liver fat in nonalcoholic fatty liver disease trials: Hepatology. Hepatology. dicembre 2013;58(6):1930–40. doi:10.1002/hep.26455

38. Rockey DC, Caldwell SH, Goodman ZD, Nelson RC, Smith AD. Liver biopsy†. Hepatology. marzo 2009;49(3):1017–44. doi:10.1002/hep.22742

39. Castera L, Friedrich-Rust M, Loomba R. Noninvasive Assessment of Liver Disease in Patients With Nonalcoholic Fatty Liver Disease. Gastroenterology. aprile 2019;156(5):1264-1281.e4. doi:10.1053/j.gastro.2018.12.036

40. Hernaez R, Lazo M, Bonekamp S, Kamel I, Brancati FL, Guallar E, et al. Diagnostic accuracy and reliability of ultrasonography for the detection of fatty liver: A meta-analysis. Hepatology. 2 settembre 2011;54(3):1082–90. doi:10.1002/hep.24452

41. Reeder SB, Hu HH, Sirlin CB. Proton density fat-fraction: A standardized mr-based biomarker of tissue fat concentration. Magnetic Resonance Imaging. novembre 2012;36(5):1011–4. doi:10.1002/jmri.23741

42. Tang A, Desai A, Hamilton G, Wolfson T, Gamst A, Lam J, et al. Accuracy of MR Imaging–estimated Proton Density Fat Fraction for Classification of Dichotomized Histologic Steatosis Grades in Nonalcoholic Fatty Liver Disease. Radiology. febbraio 2015;274(2):416–25. doi:10.1148/radiol.14140754

43. Li Y, Jin D, Liu S, Jiang C, Ni M, Feng L, et al. Quantification of the Proton Density Fat Fraction and Iron Content: A Comparative Study Between 3.0 T and 5.0 T MRI. Magnetic Resonance Imaging. agosto 2025;62(2):551–60. doi:10.1002/jmri.29743

44. Stine JG, Munaganuru N, Barnard A, Wang JL, Kaulback K, Argo CK, et al. Change in MRI-PDFF and Histologic Response in Patients With Nonalcoholic Steatohepatitis: A Systematic Review and Meta-Analysis. Clinical Gastroenterology and Hepatology. novembre 2021;19(11):2274-2283.e5. doi:10.1016/j.cgh.2020.08.061

45. Zhang YX, Feng YP, You CL, Zhang LY. The diagnostic value of MRI-PDFF in hepatic steatosis of patients with metabolic dysfunction-associated steatotic liver disease: a systematic review and meta-analysis. BMC Gastroenterol. 1 luglio 2025;25(1):451. doi:10.1186/s12876-025-04017-4

46. Hirooka M, Ogawa S, Koizumi Y, Yoshida Y, Goto T, Yasuda S, et al. iATT liver fat quantification for steatosis grading by referring to MRI proton density fat fraction: a multicenter study. J Gastroenterol. giugno 2024;59(6):504–14. doi:10.1007/s00535-024-02096-w

47. Ferraioli G, Roccarina D, Barr RG. Attenuation Coefficient for Hepatic Steatosis Using a Single Ultrasound System: Associations of Measurement Parameters With Interoperator Agreement and Diagnostic Performance. American Journal of Roentgenology. giugno 2025;224(6):e2532746. doi:10.2214/AJR.25.32746

48. Huang YL, Sun C, Wang Y, Cheng J, Wang SW, Wei L, et al. Ultrasound-guided attenuation parameter for identifying metabolic dysfunction-associated steatotic liver disease: a prospective study. Ultrasonography. 1 marzo 2025;44(2):134–44. doi:10.14366/usg.24204

49. Hamadouche M, Vilgrain V, Hobeika C, Castera L, Valla D, Rautou PE, et al. Ultrasound hepatorenal index for the diagnosis of steatosis in patients with type 2 diabetes: a prospective validation study. Eur Radiol. 25 giugno 2025;35(12):7927–39. doi:10.1007/s00330-025-11774-z

50. Karlas T, Petroff D, Sasso M, Fan JG, Mi YQ, De Lédinghen V, et al. Individual patient data meta-analysis of controlled attenuation parameter (CAP) technology for assessing steatosis. Journal of Hepatology. maggio 2017;66(5):1022–30. doi:10.1016/j.jhep.2016.12.022

51. Indre MG, Leucuta DC, Lupsor-Platon M, Turco L, Ferri S, Hashim A, et al. Diagnostic accuracy of 2D-SWE ultrasound for liver fibrosis assessment in MASLD: A multilevel random effects model meta-analysis. Hepatology. agosto 2025;82(2):454–69. doi:10.1097/HEP.0000000000001190

52. Xu X, Zhang Y, Zhu Q, Xie Y, Zhou Y, Dong B, et al. Diagnostic accuracy of two-dimensional shear wave elastography and point shear wave elastography in identifying different stages of liver fibrosis in patients with metabolic dysfunction-associated steatotic liver disease: A meta-analysis. Biomol Biomed. 10 gennaio 2025;25(4):810–21. doi:10.17305/bb.2024.11577

53. Yamaguchi R, Oda T, Nagashima K. Comparison of the diagnostic accuracy of shear wave elastography with transient elastography in adult nonalcoholic fatty liver disease: a systematic review and network meta-analysis of diagnostic test accuracy. Abdom Radiol. 6 settembre 2024;50(2):734–46. doi:10.1007/s00261-024-04546-8

54. Wear KA, Han A, Rubin JM, Gao J, Lavarello R, Cloutier G, et al. US Backscatter for Liver Fat Quantification: An AIUM-RSNA QIBA Pulse-Echo Quantitative Ultrasound Initiative. Radiology. dicembre 2022;305(3):526–37. doi:10.1148/radiol.220606

55. Loomba R, Cui J, Wolfson T, Haufe W, Hooker J, Szeverenyi N, et al. Novel 3D Magnetic Resonance Elastography for the Noninvasive Diagnosis of Advanced Fibrosis in NAFLD: A Prospective Study. American Journal of Gastroenterology. luglio 2016;111(7):986–94. doi:10.1038/ajg.2016.65

56. Pavlides M, Banerjee R, Sellwood J, Kelly CJ, Robson MD, Booth JC, et al. Multiparametric magnetic resonance imaging predicts clinical outcomes in patients with chronic liver disease. Journal of Hepatology. febbraio 2016;64(2):308–15. doi:10.1016/j.jhep.2015.10.009

57. Cannella R, Matteini F, Gagliano DS, Mazzola M, Agnello F, Soresi M, et al. Performance of Ultrasound Liver Fat Quantification for the Assessment of Hepatic Steatosis Using MRI Fat Fraction as a Reference Standard. Ultrasound in Medicine & Biology. settembre 2025;51(9):1495–502. doi:10.1016/j.ultrasmedbio.2025.05.020

58. Qu Y, Li M, Hamilton G, Zhang YN, Song B. Diagnostic accuracy of hepatic proton density fat fraction measured by magnetic resonance imaging for the evaluation of liver steatosis with histology as reference standard: a meta-analysis. Eur Radiol. ottobre 2019;29(10):5180–9. doi:10.1007/s00330-019-06071-5

59. Benchoufi M, Matzner-Lober E, Molinari N, Jannot AS, Soyer P. Interobserver agreement issues in radiology. Diagnostic and Interventional Imaging. ottobre 2020;101(10):639–41. doi:10.1016/j.diii.2020.09.001

60. Obesity: preventing and managing the global epidemic. Report of a WHO consultation. World Health Organ Tech Rep Ser. 2000;894:i–xii, 1–253. PubMed PMID: 11234459.

61. Paige JS, Bernstein GS, Heba E, Costa EAC, Fereirra M, Wolfson T, et al. A Pilot Comparative Study of Quantitative Ultrasound, Conventional Ultrasound, and MRI for Predicting Histology-Determined Steatosis Grade in Adult Nonalcoholic Fatty Liver Disease. American Journal of Roentgenology. maggio 2017;208(5):W168–77. doi:10.2214/AJR.16.16726

62. Gao R, Han J, Song D, Wang P, Chen H, Shen H, et al. Quantitative assessment of hepatic steatosis by ultrasound-guided attenuation parameter in patients with impaired glucose tolerance. Insights Imaging. 6 novembre 2025;16(1):247. doi:10.1186/s13244-025-02123-1

63. Ferraioli G, Maiocchi L, Raciti MV, Tinelli C, De Silvestri A, Nichetti M, et al. Detection of Liver Steatosis With a Novel Ultrasound-Based Technique: A Pilot Study Using MRI-Derived Proton Density Fat Fraction as the Gold Standard. Clin Transl Gastroenterol. 11 ottobre 2019;10(10):e00081. doi:10.14309/ctg.0000000000000081

64. Idilman IS, Aniktar H, Idilman R, Kabacam G, Savas B, Elhan A, et al. Hepatic Steatosis: Quantification by Proton Density Fat Fraction with MR Imaging versus Liver Biopsy. Radiology. giugno 2013;267(3):767–75. doi:10.1148/radiol.13121360

65. Reeder SB, Cruite I, Hamilton G, Sirlin CB. Quantitative assessment of liver fat with magnetic resonance imaging and spectroscopy. Magnetic Resonance Imaging. ottobre 2011;34(4). doi:10.1002/jmri.22775

66. Ozturk A, Kumar V, Pierce TT, Li Q, Baikpour M, Rosado-Mendez I, et al. The Future Is Beyond Bright: The Evolving Role of Quantitative US for Fatty Liver Disease. Radiology. 1 novembre 2023;309(2):e223146. doi:10.1148/radiol.223146

67. Marshall RH, Eissa M, Bluth EI, Gulotta PM, Davis NK. Hepatorenal Index as an Accurate, Simple, and Effective Tool in Screening for Steatosis. American Journal of Roentgenology. novembre 2012;199(5):997–1002. doi:10.2214/AJR.11.6677

68. Zeng KY, Bao WYG, Wang YH, Liao M, Yang J, Huang JY, et al. Non-invasive evaluation of liver steatosis with imaging modalities: New techniques and applications. World J Gastroenterol. 7 maggio 2023;29(17):2534–50. doi:10.3748/wjg.v29.i17.2534

69. Jang W, Song JS. Non-Invasive Imaging Methods to Evaluate Non-Alcoholic Fatty Liver Disease with Fat Quantification: A Review. Diagnostics. 25 maggio 2023;13(11):1852. doi:10.3390/diagnostics13111852

70. Kumada T, Toyoda H, Ogawa S, Gotoh T, Suzuki Y, Imajo K, et al. Advanced fibrosis leads to overestimation of steatosis with quantitative ultrasound in individuals without hepatic steatosis. Ultrasonography. 1 marzo 2024;43(2):121–31. doi:10.14366/usg.23194

71. Mendoza YP, Rodrigues SG, Delgado MG, Murgia G, Lange NF, Schropp J, et al. Inflammatory activity affects the accuracy of liver stiffness measurement by transient elastography but not by

two-dimensional shear wave elastography in non-alcoholic fatty liver disease. Liver International. gennaio 2022;42(1):102–11. doi:10.1111/liv.15116